J Biomol NMR (2007) 39:153–163
DOI 10.1007/s10858-007-9184-4

ARTICLE

^{13}C-detected NMR experiments for measuring chemical shifts and coupling constants in nucleic acid bases

Radovan Fiala · Vladimír Sklenář

Received: 5 June 2007 / Accepted: 20 July 2007 / Published online: 14 August 2007

Abstract The paper presents a set of two-dimensional experiments that utilize direct ^{13}C detection to provide proton–carbon, carbon–carbon and carbon–nitrogen correlations in the bases of nucleic acids. The set includes a ^{13}C-detected proton–carbon correlation experiment for the measurement of ^{13}C–^{13}C couplings, the CaCb experiment for correlating two quaternary carbons, the HCaCb experiment for the ^{13}C–^{13}C correlations in cases where one of the carbons has a proton attached, the HCC-TOCSY experiment for correlating a proton with a network of coupled carbons, and a ^{13}C-detected ^{13}C–^{15}N correlation experiment for detecting the nitrogen nuclei that cannot be detected via protons. The IPAP procedure is used for extracting the carbon–carbon couplings and/or carbon decoupling in the direct dimension, while the S^{3}E procedure is preferred in the indirect dimension of the carbon–nitrogen experiment to obtain the value of the coupling constant. The experiments supply accurate values of ^{13}C and ^{15}N chemical shifts and carbon–carbon and carbon–nitrogen coupling constants. These values can help to reveal structural features of nucleic acids either directly or via induced changes when the sample is dissolved in oriented media.

Keywords Chemical shift · Direct carbon detection · NMR · Nucleic acid · Quaternary carbon · Spin–spin coupling

Abbreviations

AP	anti-phase
DIPAP	Double IPAP
DSS	4,4-dimethyl 4-silapentane sodium sulfonate
HSQC	Heteronuclear single-quantum correlation
INEPT	Insensitive nuclei enhancement by polarization transfer
IP	In-phase
PCM	Polarizable continuum model
RDC	Residual dipolar coupling
S^{3}E	Spin-state selective excitation

Introduction

NMR chemical shifts in biological macromolecules represent an invaluable source of structural information. While the ^{13}C chemical shifts are routinely used to predict elements of the secondary structure in proteins, only the proton shieldings has been successfully correlated with the tertiary structure in DNA (Wijmenga et al. 1997) and RNA (Cromsigt et al. 2001). For now, a limited set of ^{13}C and ^{15}N data, reporting the chemical shifts of RNA and DNA oligonucletides in the BioMagResBank (http://www.bmrb.wisc.edu), hampers the effort to evaluate the influence of secondary and tertiary structures on the chemical shielding. However, it is reasonable to expect that the involvement of exchangeable protons and electron lone pairs of the aromatic systems in hydrogen bonding, together with

Electronic supplementary material The online version of this article (doi:10.1007/s10858-007-9184-4) contains supplementary material, which is available to authorized users.

R. Fiala · V. Sklenář (✉)
National Centre for Biomolecular Research, Masaryk University, Kotlářská 2, Brno 611 37, Czech Republic
e-mail: sklenar@ncbr.chemi.muni.cz

R. Fiala
e-mail: fiala@ncbr.chemi.muni.cz

changing patterns of base-to-base stacking interactions, modifies shielding of individual nuclei in a distinct manner. In order to enlarge the pool of targets for the chemical shift measurements beyond the one represented by protonated carbons and nitrogens, it is desirable to have on hand a set of experiments for the measurements of all non-protonated nuclei. The ^{15}N chemical shifts of nitrogens in purine and pyrimiden bases can be obtained by two- or three-dimensional HCN or HCNCH experiments (N1(C,U,T), N9(A,G), N1(A), N3(A)) in combination with long-range HSQC and HNN-COSY (N7(A,G), N3(C)), see (Furtig et al. 2003) for a recent review. These experiments rely on relatively large one-bond H–C (180–220 Hz) and C–N (9–13 Hz), and two-bond H–N (9–17 Hz) scalar interactions or moderate N–N couplings over two bonds or across the hydrogen bonds. Until now, non-protonated carbons, namely C2 and C4 in uracil and cytosine, C2, C4, and C5 in thymine, C4, C5, and C6 in adenine, and C2, C4, C5, and C6 in guanine (Fig. 1) attracted little attention. However, two recent studies by H. Schwalbe's (Furtig et al. 2004) and our groups (Fiala et al. 2004) proposed experiments for measuring the chemical shifts of non-protonated carbons based on double-resonance long-range HSQC and/or triple-resonance ^{1}H, ^{13}C, ^{15}N through-bond correlations. A combination of the available experiments allows measurements of all non-protonated carbons with the exception of C2 in the guanine residues that have the imino proton signals broadened beyond detection (Fiala et al. 2004). As we have shown for the U6 25-nt RNA fragment, the proton detected HSQC and ^{1}H–^{13}C–^{15}N experiments are also applicable to the measurements of chemical shifts in partially aligned oligonucleotides although with reduced sensitivity due to long evolution delays and accelerated T_2 relaxation of ^{1}H nuclei.

The introduction of cryogenic probeheads with increased sensitivity for ^{13}C (Kovacs et al. 2005; Serber et al. 2000), along with the methods developed for the decoupling of large one-bond carbon–carbon interactions (Duma et al. 2003; Shimba et al. 2003) have opened the way for the use of ^{13}C direct-detection experiments in NMR spectroscopy of biomolecules. A great variety of carbon-detected experiments has been recently proposed for NMR spectroscopy of proteins (Bermel et al. 2006c). Indeed, a strategy for a complete assignment of protein resonances using "protonless spectroscopy" (Bermel et al. 2005b, 2006a, b) has been developed for the study of systems containing paramagnetic ions or for large, fully deuterated protein molecules. The lower magnetogyric ratio of ^{2}H compared to that of ^{1}H contributes to a drastic reduction of dipole–dipole interactions and extends the lifetimes of excited carbon spin states. The lower inherent sensitivity of the carbon detection, by a factor of $(\gamma_H/\gamma_C)^{3/2} = 8$, is partially offset by avoiding the transfer of magnetization to a proton for detection, making thus the pulse sequences shorter and less prone to relaxation losses. The ^{13}C direct detection also increases the detectability of residual dipolar couplings in the cases of broadened proton resonances (Balayssac et al. 2006). Other advantages of the ^{13}C-detected experiments in proteins include high chemical shift dispersion in the carbon dimension, easy detection of non-protonated carbons, no need for solvent or buffer suppression, and lower susceptibility to the deteriorating effects of high salt concentrations on the sensitivity of NMR measurements.

In nucleic acids, however, the situation is somewhat different. Selective deuteration procedures target usually sugars (Cromsigt et al. 2002; Nikonowicz 2001; Tolbert and Williamson 1996, 1997), making fully deuterated bases with the ^{13}C labeling rare, and the high chemical shielding

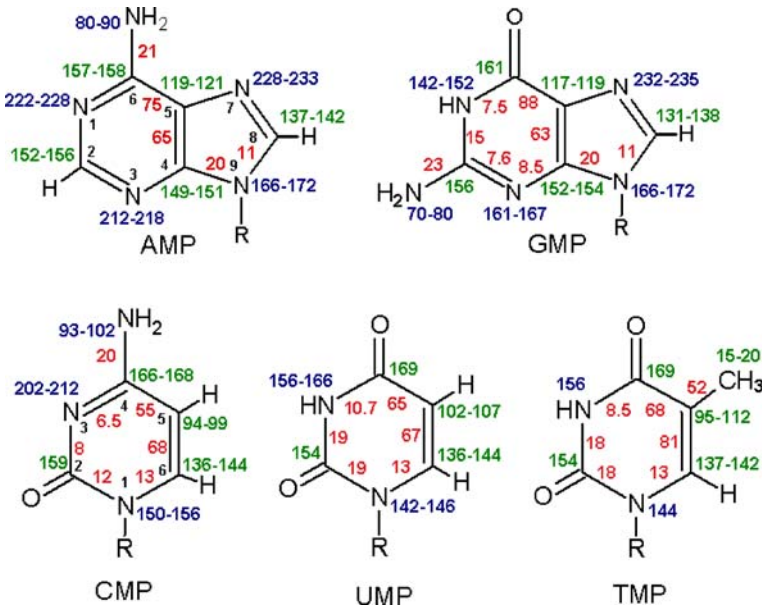

Fig. 1 Typical chemical shift ranges (ppm) of ^{13}C (green) and ^{15}N (blue) in oligonucleotides and one-bond spin–spin couplings (Hz, red) in nucleic acid bases (Wijmenga and van Buuren 1998). The coupling values were measured on mononucleotides except for T, where the values were obtained by DFT calculation in PCM solvent for thymine methylated at position 1 (Křistková A, personal communication). The couplings smaller than 5 Hz are not shown. UIPAC atom numbering (black) for purine and pyrimidine bases is given in the formulas of adenine and cytosine, respectively

anisotropy of base carbons, together with a lower proton density, diminish the role of the dipolar relaxation. Therefore, the improvement of the relaxation properties achieved with the carbon-detected approach will be less dramatic than in the proteins. Nonetheless, the bases of nucleic acids contain several non-protonated quaternary carbon atoms with potentially important structural information, which are suitable for the direct carbon detection. The spin topology in aromatic bases offers only C8s and C2s in purines and C2s in pyrimidines as the carbons free of a large, single bond ^{13}C–^{13}C scalar coupling. The network of coupled carbon spins in ^{13}C-enriched compounds causes splitting of the C4, C5, and C6 signals of both purine and pyrimidine nucleotides in the directly detected dimension. This can be seen as a disadvantage in situations when the chemical shift values are a primary target of experimental investigations. However, the ^{13}C splitting can be readily used for measuring one-bond carbon–carbon couplings.

Residual dipolar couplings and induced changes of chemical shifts, measurable in partially oriented oligonucleotides, supply a wealth of information facilitating the structure determination of nucleic acids. Since only three of their independent values can be measured within a single base, more data is desired to allow cross-validation or as a substitute for missing and/or overlapped signals (Žídek et al. 2003). A number of couplings between heteronuclei is available from proton-detected experiments (Žídek et al. 2001; Boisbouvier et al. 2004; Jaroniec et al. 2005) but many others remain inaccessible. Due to a low abundance of hydrogen atoms in nucleic acid bases it is desirable to complement data from single- and two-bond proton–carbon and proton–nitrogen NMR experiments by carbon–carbon and carbon–nitrogen values using direct ^{13}C detection.

Here we present a suite of ^{13}C-detected NMR experiments primarily designed to detect non-protonated carbons in purine and pyrimidine bases of nucleic acids that utilize direct ^{13}C detection to provide proton–carbon, carbon–carbon and carbon–nitrogen correlations. The set includes a ^{13}C-detected proton–carbon correlation experiment, the CaCb experiment for correlating two quaternary carbons, the HCaCb experiment for the cases where one of the carbons has a proton attached, the HCC-TOCSY experiment for correlating a proton with a network of coupled carbons, and a ^{13}C-detected carbon–nitrogen correlation experiment for detecting the nitrogen nuclei that cannot be detected via protons. The IPAP procedure (Andersson et al. 1998; Ottiger et al. 1998) is used for extracting the carbon–carbon couplings and/or for the carbon decoupling in the direct dimension while the S^3E procedure (Meissner et al. 1997a, b) is preferred in the indirect dimension of the carbon–nitrogen experiment to obtain the value of the coupling constant. The experiments supply accurate values of ^{13}C and ^{15}N chemical shifts and carbon–carbon and carbon–nitrogen coupling constants. Their performance is demonstrated using fully ^{13}C, ^{15}N-labeled RNA molecules with 14 and 25 nucleotides.

Materials and methods

Di-sodium salt of the ^{13}C, ^{15}N-labeled ribooligonucleotide pppGGCACUUCGGUGCC was purchased from Silantes (München, Germany). About 4 mg of the compound were dissolved in 0.55 ml of phosphate buffer containing 10% of ^2H_2O, 10 μM NaN_3 and 0.1 mM EDTA at pH 6.8 (uncorrected reading) for the final concentration of approximately 1.5 mM.

The 25-nt RNA construct related to trypanosome U6 intramolecular stem-loop with a nucleotide sequence of GGGUCUCCCUGCGCAAGGCUGAUCC, ^{13}C, ^{15}N-labeled for G and C nucleotides was synthesized by David Staple in the laboratory of Sam Butcher by in vitro transcription using purified His_6-tagged T7 RNA polymerase and synthetic DNA oligonucleotides as previously described (Reiter et al. 2003). About 0.30 ml of the sample with RNA concentration approximately 0.5 mM containing 50 mM NaCl at pH 6.8 was placed in a Shigemi NMR tube.

All NMR measurements were performed at 298 K on a 600 MHz Bruker Avance spectrometer at 14.1 T equipped with a cryogenic triple resonance (^1H, ^{13}C, ^{15}N) probe with cooled ^1H and ^{13}C preamplifiers.

Unless otherwise specified, 1024 points in the direct dimension and 128 real points in the indirect dimension were acquired for each subspectrum in the IPAP and S^3E experiments. GARP decoupling (Shaka et al. 1985) was applied as shown in the pulse schemes with the power of 2.8 kHz and 800 Hz for ^1H and ^{15}N, respectively. Other experimental details for the individual experiments are discussed further in the text. The data sets were processed in TopSpin 1.3 program into 2k × 1k matrices using square cosine apodization in both dimensions and number of points in the t_1 dimension was doubled by a linear prediction. The spectra were referenced indirectly to DSS and ammonia in the ^{13}C and ^{15}N dimensions, respectively. The carbon and nitrogen dimensions were first referenced in ^1H–^{13}C and ^1H–^{15}N correlation spectra based on the water resonance as described by (Wishart et al. 1995); the reference was then transferred to the corresponding dimensions of the ^{13}C-detected spectra run at the same conditions.

Results and discussion

The proposed experiments rely on a selective transfer of magnetization through one or more INEPT steps. Unlike in

proteins where aliphatic and carbonyl chemical shifts are well separated, the network of coupled carbon nuclei in nucleic acids is much more complicated. Therefore, a judicial choice of band-selective pulses and refocusing of unwanted interactions is essential. In all pulse sequences described, the phase sensitivity in the indirectly detected dimension is achieved by the States-TPPI method. The applied gradients serve to the artifact suppression only and do not need to be in any specific ratios.

We denote the individual experiments by the symbols for nuclei involved in the order the magnetization is transferred. The nuclei whose effect needs to be removed by selective refocusing or decoupling are given in {braces}. The atoms of the same kind are distinguished by letters in alphabetical order.

HCa{Cb} experiment

At first glance, the experiment designed to obtain one-bond ^{1}H–^{13}C correlation seems to be an unnecessary application of the ^{13}C direct detection (Fig. 2). The measurement produces ^{1}H–^{13}C correlation spectrum that carries essentially the same information as the proton-detected ^{1}H–^{13}C HSQC spectrum. The experiment consists of a two-dimensional version of the refocused INEPT pulse sequence (Burum and Ernst 1980) followed by an IPAP step for spectral editing and/or decoupling in the directly detected dimension. As the carbon-detected experiment is inherently less sensitive, the HCa{Cb} experiment is not meant as a routine replacement of the HSQC. Rather, we suggest its application in two cases:

a) Measurement of carbon–carbon coupling constants. In this experiment, the coupling is measured in the directly detected dimension. The doublets split by the carbon–carbon scalar interaction are edited in two separate subspectra avoiding increased crowding and overlap of the resonance peaks. The ^{13}C-detected experiment offers substantially higher resolution in the ^{13}C dimension over the HSQC version with the indirect proton detection. The experiment can be applied to a precise measurement of one-bond C6–C5 and C5–C4 couplings in pyrimidines.

b) Detection of ^{1}H–^{13}C correlations that are not detectable in the proton dimension due to overlap with a strong signal of water or broadening by paramagnetic ions. This is for example the case of H3′ protons in both DNA and RNA that fall in the same region as the water signal or of the proton signals in the mapping of divalent metal binding sites using Mn^{2+} as Mg^{2+} replacement. While in DNA the C3′ splitting in the ^{13}C direct dimension due to the scalar couplings to C2′ and C4′ carbons can be readily removed by IPAP with a double band-selective pulses centered at 37 and 84 ppm, respectively, in RNA, where both C2′ and C3′ carbons resonate in the same frequency range 70–78 ppm, such a procedure fails. The only possibility is to remove C3′–C4′ coupling using the band-selective C4′ pulse in the IPAP (82–86 ppm) resulting in the simplification of the C3′ coupling pattern from a triplet to a better resolved C3′–C2′ doublet. The associated ^{13}C–^{13}C coupling constant can be easily extracted benefiting from high resolution in the directly detected dimension.

Since the IP and AP experiments differ in the effect of the spin–spin coupling in the last evolution period of the pulse sequence, the phase of the resulting IP and AP signals are phase shifted by 90° (e.g. Ca_x and Ca_yCb_z coherences for IP and AP, respectively). In the original implementation of the IPAP element for homonuclear decoupling (Bermel et al. 2005a; Duma et al. 2003) the signals are brought in phase by applying a z-filter, consisting of two specifically phased 90° pulses selective to the nucleus Ca, at the end of the IPAP period. Alternatively, the phase shift in the AP spectrum relative to the IP spectrum can be eliminated by phase shifting the pulse preceding the AP period by 90° (phase φ_3 in Fig. 2). The third possibility is to correct for the phase difference between the IP and AP spectra during the processing. To avoid problems arising from the presence of additional long selective pulses while retaining the possibility of editing the data in the frequency domain, we recommend choosing the second option in most cases. The approaches

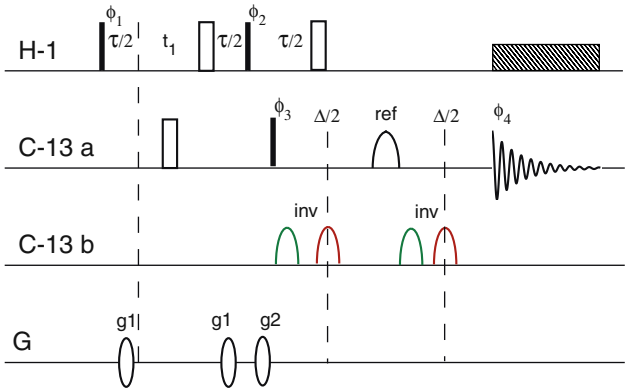

Fig. 2 Pulse sequence for HCa{Cb} experiment. Rectangular pulses are denoted by bars and amplitude modulated pulses by round symbols. The filled symbols stand for flip angles of 90° and the open symbols for flip angles of 180°. Two experiments are performed in an interleaved manner, the pulses shown in red are applied in the in-phase experiment and the green pulses in the anti-phase experiment. Optional ^{15}N decoupling during t_2 and the z-filter (see text) are not shown. The evolution intervals are $\tau = 1/(2J_{HC})$ and $\Delta = 1/(2J_{CC})$, phase cycle: φ_1 = x + States-TPPI, −x, φ_2 = y, y, −y, −y, φ_3 = 4x, 4(−x) for IP and 4y, 4(−y) for AP, φ_4 = x, −x, −x, x, −x, x, x, −x

with and without the z-filter described above are equivalent except for two notable distinctions. A nucleus without a coupling partner, such as purine C8 in our case, does not evolve into anti-phase during the IPAP period and therefore appears phase shifted by 90° with respect to the C6 peaks. After adding and subtracting the IP and AP spectra, the purine C8 peaks appear with a mixed phase which represents a sum of a correctly phased (IP) and 90° out-of-phase (AP) components. If this is a problem, the z-filter, which removes the C8 signals from the AP spectra, should be used. With the use of a z-filter, the purine C8 signals appear with a correct phase in the edited spectra, albeit with reduced intensity (Fig. 3). Similarly, the z-filter removes the out-of-phase component from the AP spectrum if the length of the IPAP period does not correspond to the value of the coupling constant. Therefore, if the dispersion of the carbon-carbon coupling constants is large and the evolution interval Δ had to be set to a compromise value, the presence of the z-filter is desirable.

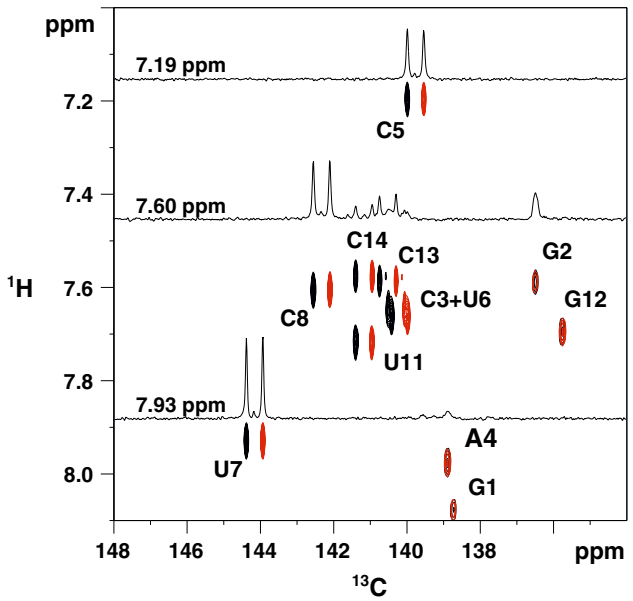

Fig. 3 Pyrimidine H6–C6 region of the HC6{C5}spectra of the UUCG hairpin. The J_{C5C6} coupling constants can be measured between the red and black peaks in the doublets. 1D traces are included to show peak shapes and phase properties. The doublets are significantly better resolved than in the corresponding proton detected spectrum coupled in t_1 (Supplementary Fig. S1). Note that the red and black peaks come from separate subspectra and do not cancel in the case of an overlap. The signals of purine C8s were removed from the AP spectrum by a z-filter (not shown in Fig. 2), therefore the corresponding peaks appear with a reduced intensity (see text for details). τ = 2.7 ms, Δ = 7.5 ms. Offsets were set to 7.8 ppm for H6, to 140 ppm for C6, and to 100 ppm for C5 with 1.0 ms Q3 band-selective pulses. The ^{15}N decoupling during t_2 was centered at 157 ppm. Spectral widths were 30 ppm in the carbon and 5 ppm in the proton dimensions. 16 scans per t_1 increment resulted in the total experimental time of two and a half hours

An S^3E element (Meissner et al. 1997a, b) can be used instead of the IPAP approach for spectral editing and homonuclear decoupling (Bermel et al. 2005a, 2006c). The main difference between the two approaches is that the duration of the S^3E element is half that of IPAP. The S^3E element is therefore more suitable if the evolution intervals are long and the relaxation is a concern. Since the values of one-bond carbon–carbon couplings in nucleic acid bases are large and pulses involved have to be highly selective, we prefer the IPAP approach for the carbon–carbon editing. The IPAP procedure has also been reported as more robust with respect to the variations of the coupling constants involved (Brutscher 2001). On the other hand, for spectral editing based on much smaller carbon–nitrogen couplings, use of the S^3E approach reduces the length of the pulse sequence significantly and is essential for obtaining sufficient sensitivity.

Ca{Cc}Cb{Ca} experiment

The experiment is suitable for correlating a carbon nucleus, which has two coupling partners, with one of the partners and for measuring their coupling constant, for example C5–C4 and J_{C5C4} in purines and in thymine. The experiment is easier to perform in the pyrimidine nucleotides where the C5 (95–110 ppm), C6 (136–144 ppm), and C4 (165–170 ppm) nuclei resonate in distinct, well separated regions. In this case, the pulse sequence is similar to the CACO experiment proposed for proteins with refocusing pulses added to remove the effect of the other coupling partner in the t_1 dimension (see Supplementary Material for details). Compared to pyrimidines, the carbon–carbon coupling constants in the C4–C5–C6 moiety of the purine bases are larger ($J_{C5C6} \sim 90$ Hz, and $J_{C4C5} \sim 60$ Hz) leading to shorter evolution intervals. The difference in the chemical shifts of C4 (149–154 ppm) and C6 (157–161 ppm) is much smaller, resulting in significantly longer selective pulses. Therefore, elements of pulse sequences with a number of pulses within one evolution interval are difficult to implement. This for example prevents the transfer of magnetization from C4 and C6 to C5 carbon with a subsequent DIPAP editing. Measurements at very high field (>18.7 T) will partially alleviate this problem. To achieve the C5–C4 and C5–C6 correlations in purines at 14.1 T, we have adopted a less selective approach (Fig. 4). In the case of the C5–C6 transfer, we took advantage of the fact that $J_{C5C6} \sim 90$ Hz and $J_{C5C4} \sim 60$ Hz are approximately in the ratio 3:2. By setting the evolution interval Δ to $3/(2J_{C5C6})$ = 16.3 ms, the evolution of the antiphase term $C5_yC4_z$ is effectively eliminated. Obviously, there is no equivalent setting for the C5–C4 correlation, which would suppress the C5–C6 transfer in a similar manner. In

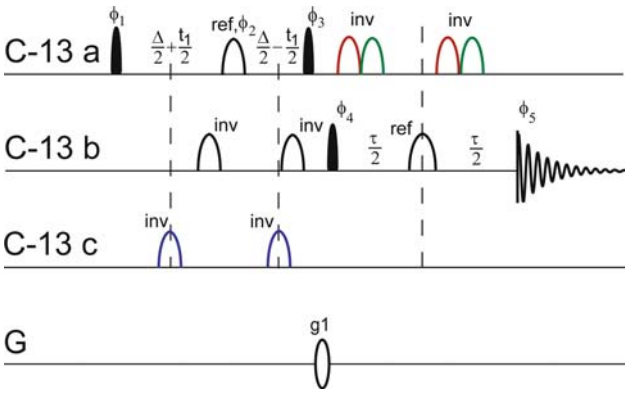

Fig. 4 Pulse sequence for Ca{Cc}Cb{Ca} experiment. The filled symbols stand for flip angles of 90° and the open symbols for flip angles of 180°. Two experiments are performed in an interleaved manner, the pulses shown in red are applied in the in-phase experiment and the green pulses in the anti-phase experiment. The evolution interval Δ is set to $1/(2J_{CaCb})$, phase cycle: φ_1 = x, −x + States-TPPI, φ_2 = 4x, 4(−x), φ_3 = y, φ_4 = x, x, −x, −x for IP and −y, −y, y, y for AP, φ_5 = x, −x, −x, x, −x, x, x, −x. ^{1}H and ^{15}N decoupling (not shown in the scheme) can be used during t_1 and t_2 if necessary. For purine C5–C6 correlation, the pulses on Cc≡C4 (blue) were omitted and Δ was set to 16.6 ms, corresponding to $(3/2J_{C5C6})$ and $(1/J_{C4C5})$. For purine C5–C4 correlation, a non-selective refocusing C5 pulse was applied, the inversion pulses on C4 were omitted and Δ was set to 24.45 ms. C5 offset was set to 118 ppm, C6 offset to 160 ppm, and C4 offset to 150 ppm. As selective pulses, 1.2 ms Q5 (Q5tr for the pulse with phase φ_3) were used for 90° pulses and 1.0 ms Q3 for 180° pulses

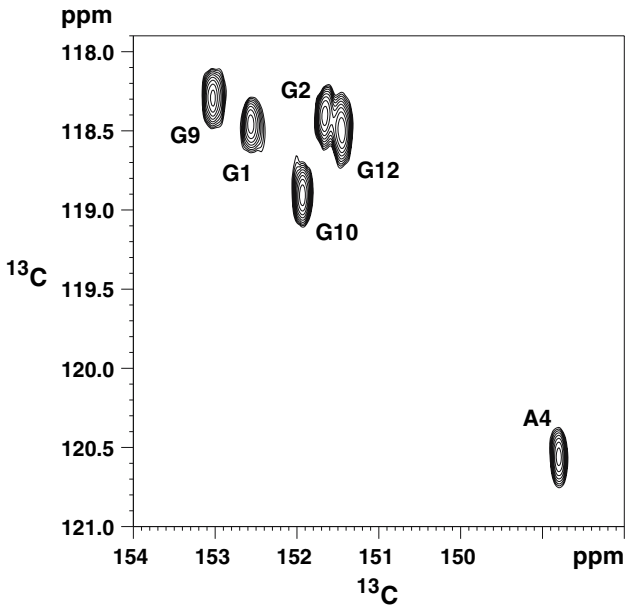

Fig. 5 Purine C5–C4 region of the C5{C6}C4{C5} spectrum of the UUCG hairpin. The spectrum was decoupled in the direct dimension by adding the IPAP edited subspectra shifted by 65 Hz. The same subspectra can be used to measure the J_{C5C4} coupling constants. The constant time evolution interval Δ was set to 24.45 ms $(3/2J_{C4C5})$ and τ to 8.3 ms $(1/2J_{C4C5})$, offsets for C4 to150 ppm, for C5 to 118 ppm, and for C6 to 160 ppm. The ^{15}N decoupling was centered at 157.5 ppm. Spectral width was 30 ppm in both dimensions and the total experimental time 5 h with 32 scans per t_1 increment

this case, we used a nonselective transfer with selective refocusing of the C6 magnetization. To increase the t_1 acquisition time and improve the F1 resolution, the constant time value of $3/(2J_{C5C4})$ = 25 ms is used as the nonselective approach does not allow the semi-constant time t_1 incrementation. The C5C4 correlation spectrum of the UUCG hairpin (Fig. 5) shows an adenine peak at 148.8 ppm clearly separated from five guanine peaks between 151.0–153.5 ppm. The spectrum has been decoupled in the direct dimension by adding and shifting the IP and AP spectra. The edited subspectra (not shown) can be used to measure the values of J_{C5C4}. This coupling is potentially very valuable for measuring RDCs since there is no other large one-bond coupling parallel to the C4C5 bond in the purine bases.

HCa{Cc}Cb{Ca} experiment

The experiment (Fig. 6) provides a correlation of quaternary carbons with protons attached to the neighboring carbon and with the presence of another interfering carbon. As an example, the correlation of H5s to C4s and the measurement of one-bond carbon–carbon coupling constants J_{C4C5} in the uracil and cytosin H5C5{C6}C4{C5} spin system is shown (Fig. 7). The information content is similar to that of the C5{C6}C4{C5} spectra described above, the difference being ^{1}H chemical shifts of H5 in the t_1 dimension instead of the shifts of the C5 nucleus. While the carbon chemical shifts often exhibit better dispersion with less overlap compared to the proton dimension (compare the spectrum in Fig. 7 with the C5–C4 correlation spectrum in supplementary Fig. S3), the HC5{C6}C4{C5} experiment is noticeably more sensitive since it starts from ^{1}H polarization, which is four times higher compared to the ^{13}C polarization. Slight differences in the intensities of the two doublet components are caused by cross-correlation between the C4–C5 dipole–dipole coupling and the C4 chemical shift anisotropy (Riek et al. 2001). To avoid technical problems with overlapping pulses during the C5C4 evolution interval, the selective polarization transfer between the carbon nuclei was implemented by using a non-selective 180° pulse in the middle of the Δ interval and by selective refocusing of the C5C6 coupling.

HCC-TOCSY experiment

All purine carbons, except for C5, fall within a band of approximately 30 ppm and can be correlated to the H8 protons and/or adenine H2 protons using the TOCSY-type

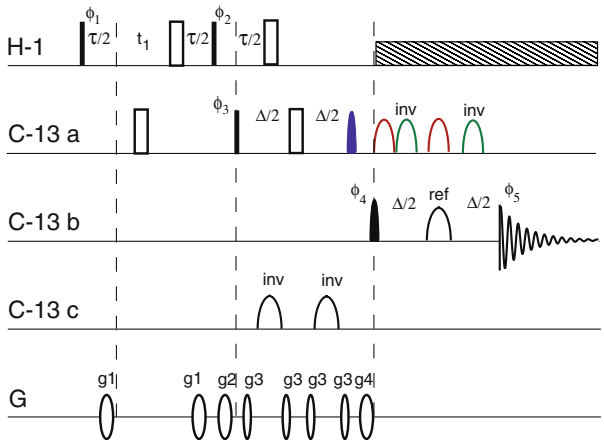

Fig. 6 Pulse sequence for HCa{Cc}Cb{Ca} experiment. Rectangular pulses are denoted by bars and amplitude modulated pulses by round symbols. The filled symbols stand for flip angles of 90° and the open symbols for flip angles of 180°. Two experiments are performed in an interleaved manner, the pulses shown in red are applied in the in-phase experiment and the green pulses in the anti-phase experiment. Optional ^{15}N decoupling during t_2 is not shown. The evolution intervals are $\tau = 1/(2J_{HCa})$ and $\Delta = 1/(2J_{CaCb})$, phase cycle: φ_1 = x, −x + States-TPPI, φ_2 = y, y, −y, −y, φ_3 = 4x, 4(−x), φ_4 = 8y, 8(−y) for IP, 8x, 8(−x) for AP, φ_5 = x, −x, −x, x, −x, x, x, −x, −x, x, x, −x, x, −x, −x, x

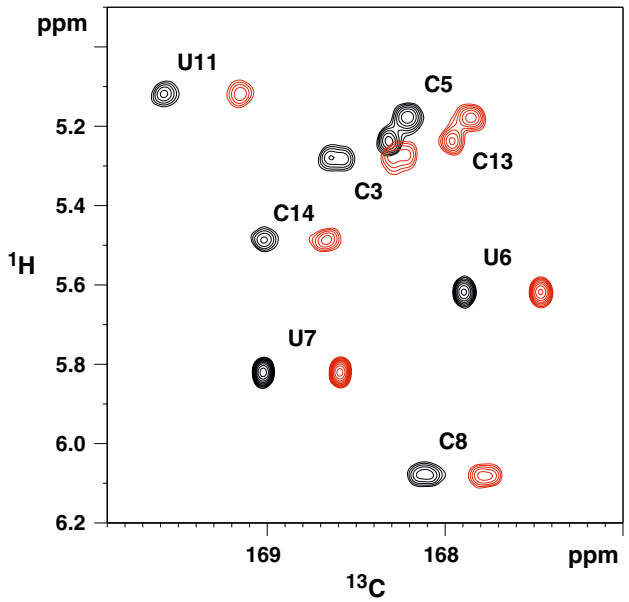

Fig. 7 Pyrimidine H5–C4 region of the HC5{C6}C4{C5} spectra of the UUCG hairpin. The J_{C5C4} coupling constants can be measured between the red and black peaks in the doublets. Note that the red and black peaks come from separate subspectra and do not cancel in the case of an overlap. Evolution intervals τ = 2.7 ms and Δ = 7.7 ms were optimized for uracil. Offsets were set to 5.8 ppm for H5, 167 ppm for C4, 100 ppm for C5, and 140 ppm for C6. Offset for Ca ≡ C5 was set to100 ppm, for Cb ≡ C4 to 167, and for Cc ≡ C6 to 140 ppm. 1 ms Q3 pulses were used for both selective inversion and refocusing and 1.25 ms Q5 (black) or Q5tr (blue) as 90° pulses. Spectral widths were 30 ppm in the carbon and 5 ppm in the proton dimensions. The total experimental time was 2.5 hours using 16 scans per t_1 increment

transfer (Fig. 8). The pulse sequence developed for the protein samples (Serber et al. 2001) can be used with the carbonyl refocusing pulses omitted. In short, H8/H2 magnetization is transferred to C8/C2 by an INEPT step, which is highly efficient thanks to a large one-bond J_{CH}. The $C8/2_yH8/2_z$ magnetization is refocused and the resulting $C8/2_x$ magnetization is then transfered by TOCSY-type mixing to other carbon nuclei where it is detected. In our implementation, we used FLOPSY16 mixing sequence (Kadkhodaie et al. 1991), which has been shown to be the most efficient one for ^{13}C broad-band homonuclear cross-polarization (Mohebbi and Shaka 1991). The efficiency of magnetization transfer in the rather complex system of coupled carbons in purine bases has been subject of an analysis (Wijmenga and van Buuren 1998). In general, the transfer efficiency depends on the length of the mixing time, on the spin-lock power as well as on the relaxation properties of the molecule. Rather long mixing of 50–70 ms is required for magnetization transfer from C8 all the way up to C6 carbons. It should be noted that the quaternary carbons primarily involved in this experiment relax more slowly than the protons or the proton carrying carbons. The pulse sequence takes advantage of starting with the high polarization of proton to improve the sensitivity. However, due to the distribution of the signal among the multiple sites and splitting of the peaks by carbon–carbon couplings, the sensitivity of the experiment is lower compared to the other carbon-detected experiments. Because the splitting of the peaks is caused by different coupling partners, the use of IPAP for decoupling in the direct dimension is not possible.

^{13}C-detected carbon–nitrogen correlation

^{13}C–^{15}N correlation spectra can be obtained using a selective version of the HSQC pulse sequence (Fig. 9) with IPAP editing for carbon decoupling and/or J_{CC} measurements in the direct dimension. An S^3E element can be incorporated in the indirect dimension for measuring carbon–nitrogen couplings. As the carbon–carbon couplings are typically much larger than carbon–nitrogen couplings, the carbon IPAP step easily fits within the last refocusing period. On the other hand, the editing step in the t_1 dimension represents an extra delay in the pulse sequence whose length should be kept to a minimum. Therefore, the use of S^3E type of editing is essential. Still, the sensitivity of S^3E edited spectra is noticeably lower that that of the spectra not edited in the t_1 dimension. The chemical shifts of the nitrogens involved in base pairing are sensitive to the character of the hydrogen bond. This is exemplified in Fig. 10a showing the C4–N4

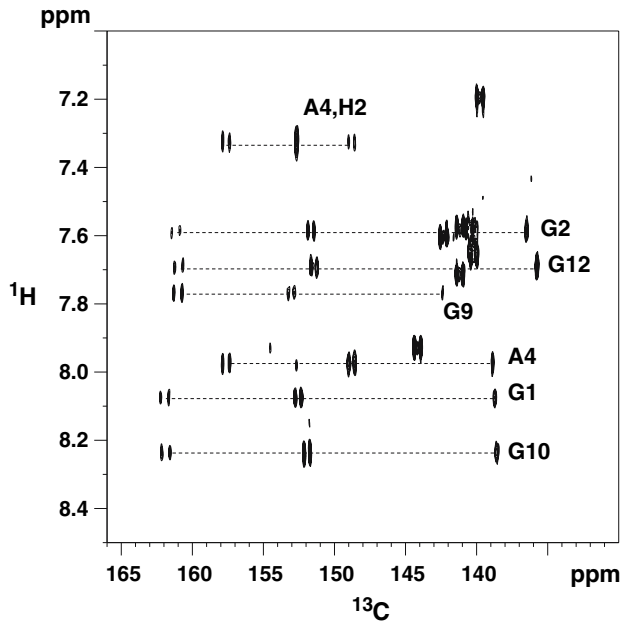

Fig. 8 Correlation of purine H8 protons with C8 (135–140 ppm), C4 (148–155 ppm) and C6 (157–163 ppm) carbons in UUCG hairpin using HCC-TOCSY. Adenine H2 correlations to C2, C4 and C6 also appear in the spectrum. Unlabeled peaks between 140 ppm and 145 ppm in the carbon dimension originate from C6 of pyrimidines. FLOPSY16 mixing at 2.15 kHz for 65.6 ms was used, proton–carbon transfer was optimized for J_{HC} = 220 Hz. The offsets were set to 7.8 ppm for proton, to 146 ppm for carbon, and 120 ppm for nitrogen. The spectral width was 40 ppm in the carbon and 3 ppm in the proton dimensions. 1024 × 100 real points were collected with 128 scans per t_1 increment giving the total experimental time 7 h

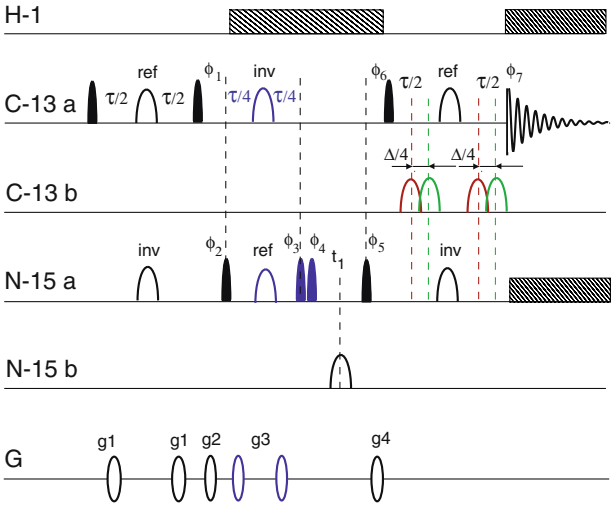

Fig. 9 Pulse sequence for CN-HSQC-S^{3}E-IPAP experiment. All pulses are preferably applied as bandselective; the filled symbols stand for flip angles of 90° and the open symbols for flip angles of 180°. Four experiments are needed for editing in both dimensions; in many cases, either the S^{3}E element (shown in blue) or the IPAP pulses (red and green) can be left out. The evolution intervals are $\tau = 1/(2J_{CN})$ and $\Delta = 1/(2J_{CaCb})$, phase cycle: φ_1 = y, y, −y, −y, $\varphi_2 = \pi/4$, $\pi/4$ for experiment A and $5\pi/4$, $5\pi/4$ for experiment B, φ_3 = x, y, φ_4 = x, y for experiment A and −x, −y for experiment B, φ_5 = x decremented in States-TPPI manner, φ_6 = x for IP and y for AP experiment, φ_7 = x, −x, −x, x. If the S^{3}E element is omitted, φ_2 = x, −x. For IP experiment, the pulses to Cb are applied in the middle of the $\tau/2$ periods and for AP are shifted by $\Delta/4$

correlation spectrum of cytosines in U6 ISL. The chemical shifts of the amino nitrogens clearly distinguish the residues in the loop from those in the stem forming base pairs. The signals from the cytidines, presumed to form a mismatched base pair, are missing. We assume that chemical shifts of these two residues moved outside the band excited by the selective pulses used or were broadened beyond detection by dynamic processes. While most of the cytosine amino nitrogens can be observed in ^{1}H–^{15}N HSQC spectra due to relatively slow exchange of amino protons, the observation of –NH_2 groups in guanines and adenines is mostly impossible. The exchange rate of ^{1}H nuclei broadens the proton signals beyond the detection limit, especially for guanines. In favorable cases, the exchange broadening of adenine amino protons can be suppressed using a CPMG mixing in the INEPT step (Mueller et al. 1995). Nevertheless, this approach fails for amino groups in guanines. As shown here, the guanine amino nitrogens N2 with exchange broadened protons can be detected via directly bonded carbons C2 (Fig. 10b). Resolution in this correlation is limited by the dispersion of the guanine C2 resonances. In the spectrum, we observe all eight signals from the guanine residues in the molecule. The peaks were tentatively assigned using the H1–N1–C2 correlation (not shown) and the assignments of imino protons from the 2D NOE spectrum. An S^{3}E editing step has been included to facilitate the measurements of ^{13}C–^{15}N coupling constants and to remove a possible overlap. In general, the ^{13}C–^{15}N splitting is too small to be resolved in 2D ^{15}N–^{13}C correlation spectra measured without a ^{13}C decoupling in the t_1 evolution period. The measurement of guanine J_{C2N2} in the UUCG hairpin is shown in Supplementary Material as Fig. S4.

Accuracy and precision of measured couplings

The accuracy and precision of measured scalar and dipolar couplings is subject to both systematic and random errors. In the case of IPAP and S^{3}E edited spectra, the measured positions of the peaks depend mainly on the correct setting of the evolution intervals in the editing filters, on the linewidths of the peaks, their correct phasing, and on the signal-to-noise ratio in the spectra. The distribution of coupling constants inevitably leads to cross-talks between α- and β-edited subspectra. Fortunately, a correction for the effect is possible during the processing (Meissner et al. 1998; Žídek et al. 2001). The effects of the noise and phase correction depend mainly on the line width. For the

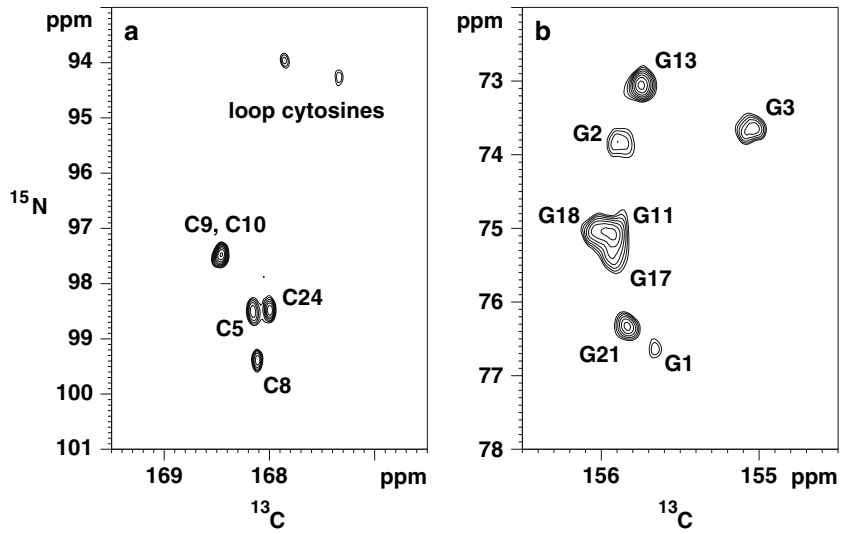

Fig. 10 Cytosine C4–N4 (**a**) and guanine C2–N2 (**b**) regions of a CN-HSQC spectrum of U6 ISL. The evolution intervals were τ = 17.8 ms and Δ = 9.1 ms, the excitation offsets were set for proton decoupling to 6.5 ppm, for Ca≡C4 Cyt & C2 Gua to 160 ppm, for Cb≡C5 Cyt to 95 ppm, and for Na≡N4 Cyt & N2 Gua to 85 ppm. The Nb pulse was not applied. Spectral widths of 30 ppm in the carbon and 34 ppm in the nitrogen dimensions were applied. Nonselective 90° pulses and 1.0 ms Reburp (ref) or IBurp2 (inv) pulses were used The spectral regions for cytosines and guanines were processed separately with (**a**) and without (**b**) ^{13}C IPAP decoupling, respectively. Total experimental time was 10 h with 64 scans per t_1 increment

measurement of carbon–carbon couplings, the situation is favorable, since the FIDs are collected in the direct dimension in the ^{13}C-detected experiments. This allows using sufficiently long acquisition times leading to line widths limited only by the relaxation times, which are typically longer for unprotonated carbons. It is difficult to quantify the phase correction errors since the phasing procedure is highly individual. The random errors caused by the presence of noise in the spectra can be evaluated from the repeated measurements. For the HCa{Cb}and HCa{Cb}Cc{Ca} spectra (Fig. 3, 7), the precision better than 0.1 Hz was achieved with the experimental parameters shown. The situation is less favorable in the case of the CN-HSQC-S^{3}E experiment, where the editing is performed in the indirect dimension and the sensitivity of the experiment is lower. Moreover, carbon–nitrogen dipolar couplings are typically only about 2–3 Hz, which increases the requirements on the precision and accuracy of the measured couplings. Therefore, to obtain the couplings with errors on the order of 0.25 Hz or better, to make them useful in the structure determination, is possible only in favorable cases of slowly relaxing nitrogens (T_2 50 ms or longer) and samples with good concentration providing high signal-to-noise ratio (30 or more).

Conclusions

We present a set of two-dimensional ^{13}C-detected correlation experiments for measuring chemical shifts and carbon–carbon and carbon–nitrogen couplings in nucleic acids. This information is potentially valuable for the structure determination. The number of available structural restraints in nucleic acids is negatively influenced by a low proton density, which is only one third compared to proteins of a similar size. Low proton density and elongated shape of the majority of structures accounts for a lack of long-range NOE restraints between the distant elements of secondary structures. Lower proton density also results in lower number of the available proton–carbon and proton–nitrogen residual dipolar couplings. Specifically, in the bases of nucleic acids only two independent one-bond ^{1}H–^{15}N or ^{1}H–^{13}C couplings are available per base at most and only one in guanine if the imino proton is not detectable. This is clearly not sufficient even assuming that the base planes are perfectly flat. Since at least three independent couplings are needed to define the base position and preferably at least one or two more couplings are required to allow crossvalidation (Žídek et al. 2003), measuring of the couplings between the heteroatoms becomes a necessity. Consequently, any additional information extracted from accurate values of the residual dipolar couplings between non-protonated ^{13}C and ^{15}N nuclei, which are not accessible using experiments with the indirect detection, could be extremely rewarding. Those couplings can be easily measured in carbon-detected spectra with improved resolution in the direct dimension. Both coupling constants and chemical shifts of ^{13}C and ^{15}N are affected in a distinct manner by changes in the hydrogen bonding and stacking interactions. Such changes

are demonstrated here for two examples of structural arrangements departing from a regular helical Watson-Crick architecture, namely for UUCG tetraloop and GCGCA loop of U6 with two unpaired Cs.

The sensitivity of the ^{13}C-detected experiments is inherently lower than of those with proton detection. However, the sensitivity disadvantage of the carbon-detected experiments is partially offset for samples dissolved in oriented media where the measurements using proton-detection suffer by a broadening of proton resonances due to the amplified ^{1}H–^{1}H dipolar interactions. As demonstrated here, modern cryogenic probe technology, in combination with high magnetic fields, makes the carbon-detected experiments feasible on real-life samples of oligonucleotides with tens of residues in the one millimolar concentration range.

Acknowledgments The work was supported by the grants MSM0021622413 to RF and LC06030 to VS provided by the Ministry of Education of the Czech Republic and by the FSG-V-RNA project of the 6th Framework Program of the European Union, Contract No. 503455. We are indebted to David Staple and Sam Butcher for the U6 ISL sample, to Wolfgang Bermel and Helena Kovacs for stimulating discussions and help in the implementation of the pulse sequences, and to Petr Novák for an assistance in the evaluation of scalar couplings.

References

Andersson P, Weigelt J, Otting G (1998) Spin-state selection filters for the measurement of heteronuclear one-bond coupling constants. J Biomol NMR 12:435–441

Balayssac S, Bertini I, Luchinat C, Parigi G, Piccioli M (2006) ^{13}C direct detected NMR increases the detectability of residual dipolar couplings. J Am Chem Soc 128:15042–15043

Bermel W, Bertini I, Duma L, Felli IC, Emsley L, Pierattelli R, Vasos PR (2005a) Complete assignment of heteronuclear protein resonances by protonless NMR spectroscopy. Angew Chem Intl Ed 44:3089–3092

Bermel W, Bertini I, Felli IC, Pierattelli R, Vasos PR (2005b) A selective experiment for the sequential protein backbone assignment from 3D heteronuclear spectra. J Magn Reson 172:324–328

Bermel W, Bertini I, Felli IC, Kummerle R, Pierattelli R (2006a) Novel ^{13}C direct detection experiments, including extension to the third dimension, to perform the complete assignment of proteins. J Magn Rerson 178:56–64

Bermel W, Bertini I, Felli IC, Lee YM, Luchinat C, Pierattelli R (2006b) Protonless NMR experiments for sequence-specific assignment of backbone nuclei in unfolded proteins. J Am Chem Soc 128:3918–3919

Bermel W, Bertini I, Felli IC, Piccioli M, Pierattelli R (2006c) ^{13}C-detected protonless NMR spectroscopy of proteins in solution. Prog NMR Spectrosc 48:25–45

Boisbouvier J, Bryce DL, O'Neil-Cabello E, Nikonowicz EP, Bax A (2004) Resolution-optimized NMR measurement of $^{1}D_{CH}$, $^{1}D_{CC}$ and $^{2}D_{CH}$ residual dipolar couplings in nucleic acid bases. J Biomol NMR 30:287–301

Brutscher B (2001) Accurate measurement of small spin-spin couplings in partially aligned molecules using a novel J-mismatch compensated spin-state-selection filter. J Magn Reson 151:332–338

Burum DP, Ernst RR (1980) Net polarization transfer via a J-ordered state for signal enhancement of low-sensitivity nuclei. J Magn Reson 39:163–168

Cromsigt J, Hilbers CW, Wijmenga SS (2001) Prediction of proton chemical shifts in RNA. Their use in structure refinement and validation. J Biomol NMR 21:11–29

Cromsigt J, Schleucher J, Gustafsson T, Kihlberg J, Wijmenga S (2002) Preparation of partially ^{2}H/^{13}C-labelled RNA for NMR studies. Stereo-specific deuteration of the H5″ in nucleotides. Nucleic Acids Res 30:1639–1645

Duma L, Hediger S, Lesage A, Emsley L (2003) Spin-state selection in solid-state NMR. J Magn Reson 164:187–195

Fiala R, Munzarová ML, Sklenář V (2004) Experiments for correlating quaternary carbons in RNA bases. J Biomol NMR 29:477–490

Fürtig B, Richter C, Wohnert J, Schwalbe H (2003) NMR spectroscopy of RNA. Chembiochem 4:936–962

Fürtig B, Richter C, Bermel W, Schwalbe H (2004) New NMR experiments for RNA nucleobase resonance assignment and chemical shift analysis of an RNA UUCG tetraloop. J Biomol NMR 28:69–79

Jaroniec CP, Boisbouvier J, Tworowska I, Nikonowicz EP, Bax A (2005) Accurate measurement of ^{15}N–^{13}C–13 residual dipolar couplings in nucleic acids. J Biomol NMR 31:231–241

Kadkhodaie M, Rivas O, Tan M, Mohebbi A, Shaka AJ (1991) Broadband homonuclear cross polarization using flip-flop spectroscopy. J Magn Reson 91:437–443

Kovacs H, Moskau D, Spraul M (2005) Cryogenically cooled probes—a leap in NMR technology. Prog NMR Spectrosc 46:131–155

Meissner A, Duus JØ, Sørensen OW (1997a) Integration of spin-state-selective excitation into 2D NMR correlation experiments with heteronuclear ZQ/2Q p rotations for $^{1}J_{XH}$-resolved E.COSY-type measurement of heteronuclear coupling constants in proteins. J Biomol NMR 10:89–94

Meissner A, Duus JØ, Sørensen OW (1997b) Spin-state-selective excitation. Application for E.COSY-type measurement of J_{HH} coupling constants. J Magn Reson 128:92–97

Meissner A, Schulte-Herbruggen T, Sørensen OW (1998) Relaxation artifacts and their suppression in multidimensional E.COSY-type NMR experiments for measurement of J coupling constants in ^{13}C- or ^{15}N-labeled proteins. J Am Chem Soc 120:7989–7990

Mohebbi A, Shaka AJ (1991) Improvements in ^{13}C broad-band homonuclear cross-polarization for 2D and 3D NMR. Chem Phys Lett 178:374–378

Mueller L, Legault P, Pardi A (1995) Improved RNA structure determination by detection of NOE contacts to exchange-broadened amino protons. J Am Chem Soc 117:11043–11048

Nikonowicz EP (2001). Preparation and use of ^{2}H-labeled RNA oligonucleotides in nuclear magnetic resonance studies. Meth Enzymol 338:320–341

Ottiger M, Delaglio F, Bax A (1998) Measurement of J and dipolar couplings from simplified two-dimensional NMR spectra. J Magn Reson 131:373–378

Reiter NJ, Nikstad LJ, Allmann AM, Johnson RJ, Butcher SE (2003) Structure of the U6 RNA intramolecular stem-loop harboring an S-P-phosphorothioate modification. RNA 9:533–542

Riek R, Pervushin K, Fernandez C, Kainosho M, Wuthrich K (2001) [^{13}C,^{13}C]- and [^{13}C,^{1}H]-TROSY in a triple resonance experiment for ribose-base and intrabase correlations in nucleic acids. J Am Chem Soc 123:658–664

Serber Z, Richter C, Dotsch V (2001) Carbon-detected NMR experiments to investigate structure and dynamics of biological macromolecules. Chembiochem 2:247–251

Serber Z, Richter C, Moskau D, Bohlen JM, Gerfin T, Marek D, Haberli M, Baselgia L, Laukien F, Stern AS, Hoch JC, Dotsch V (2000) New carbon-detected protein NMR experiments using CryoProbes. J Am Chem Soc 122:3554–3555

Shaka AJ, Barker PB, Freeman R (1985) Computer-optimized decoupling scheme for wideband applications and low-level operation. J Magn Reson 64:547–552

Shimba N, Stern AS, Craik CS, Hoch JC, Dotsch V (2003) Elimination of ^{13}C alpha splitting in protein NMR spectra by deconvolution with maximum entropy reconstruction. J Am Chem Soc 125:2382–2383

Tolbert TJ, Williamson JR (1996) Preparation of specifically deuterated RNA for NMR studies using a combination of chemical and enzymatic synthesis. J Am Chem Soc 118:7929–7940

Tolbert TJ, Williamson JR (1997) Preparation of specifically deuterated and ^{13}C-labeled RNA for NMR studies using enzymatic synthesis. J Am Chem Soc 119:12100–12108

Wijmenga SS, Kruithof M, Hilbers CW (1997) Analysis of ^{1}H chemical shifts in DNA: assessment of the reliability of H-1 chemical shift calculations for use in structure refinement. J Biomol NMR 10:337–350

Wijmenga SS, van Buuren BNM (1998) The use of NMR methods for conformational studies of nucleic acids. Prog Nucl Magn Reson Spectrosc 32:287–387

Wishart DS, Bigam CG, Yao J, Abildgaard F, Dyson HJ, Oldfield E, Markley JL, Sykes BD (1995) ^{1}H, ^{13}C and ^{15}N chemical-shift referencing in biomolecular NMR. J Biomol NMR 6:135–140

Žídek L, Wu HH, Feigon J, Sklenář V (2001) Measurement of small scalar and dipolar couplings in purine and pyrimidine bases. J Biomol NMR 21:153–160

Žídek L, Padrta P, Chmelík J, Sklenář V (2003) Internal consistency of NMR data obtained in partially aligned biomacromolecules. J Magn Reson 162:385–395